Hard limits on the postselectability of optical graph states

Jeremy C. Adcock[1], Sam Morley-Short[1], Joshua W. Silverstone*[1], and Mark G. Thompson[1]

[1]*QETLabs, H. H. Wills Physics Laboratory & Department of Electrical and Electronic Engineering, University of Bristol, Merchant Venturers Building, Woodland Road, Bristol BS8 1UB, UK*

June 2018

Coherent control of large entangled graph states enables a wide variety of quantum information processing tasks, including error-corrected quantum computation. The linear optical approach offers excellent control and coherence, but today most photon sources and entangling gates—required for the construction of large graph states—are probabilistic and rely on postselection. In this work, we provide proofs and heuristics to aid experimental design using postselection. We derive a fundamental limitation on the generation of photonic qubit states using postselected entangling gates: experiments which contain a cycle of postselected gates cannot be postselected. Further, we analyse experiments that use photons from postselected photon pair sources, and lower bound the number of classes of graph state entanglement that are accessible in the non-degenerate case—graph state entanglement classes that contain a tree are are always accessible. Numerical investigation up to 9-qubits shows that the proportion of graph states that are accessible using postselection diminishes rapidly. We provide tables showing which classes are accessible for a variety of up to nine qubit resource states and sources. We also use our methods to evaluate near-term multi-photon experiments, and provide our algorithms for doing so.

1 Introduction

Postselective linear optics has been a testbed for fundamental quantum phenomena since its inception [1–6] and although it has been shown that large-scale linear-optical quantum computing is possible in principle, it requires mid-computation measurement and feed-forward [7–10]. Modern schemes rely on the generation of large entangled states, on which measurement-based quantum computation is performed [11]. Integrated quantum photonics [12–14] is one exciting route to these goals, however it requires the on-chip generation of many-qubit quantum states.

Photons are notoriously difficult to both produce and interact on-demand. This has led to slow improvements in photon number [6, 15–19]. Today, the most common way to produce quantum states of light is to use entangled postselected pair sources (EPP sources), such those based on parametric down-conversion or spontaneous four-wave mixing. These processes can produce pair-wise entanglement and have been ubiquitous in quantum photonic information experiments over the last 30 years [5, 20–22].

Large entangled states remain a challenge to produce. Two popular ways of generating entanglement in linear optics are the postselected controlled-Z (CZ) gate [23, 24], and the postselected fusion gate [25]. So far, up to ten photons have been entangled in this way [19], though there are proposals for much larger schemes [26, 27].

Probabilistic gates are provably the only way to generate entanglement using linear optics [7], and are a central component to modern linear-optical quantum computing proposals [8–10, 28]. Currently, postselected entangling gates (PEGs) are the only way to test linear optical devices and techniques in the multi-photon regime. The complexity of generating graph-states using linear optics has not yet been analysed [29, 30].

In comparison to this work, refs. 31, 32 uses graph theory to analytically discern which high-dimensional Greenberger-Horne-Zeilinger state is produced by any assembly of nonlinear pair soureces. To do this, they use graphs where vertices correspond to optical paths, rather than qubits.

Here, we discuss entangling gates and photon-pair sources that are postselected, in which all input photons compose the final quantum state. We analyse connected graph states of "dual-rail" photonic qubits. We show that postselected gates, as well as having exponential time complexity, have a fundamental restriction on which types of entanglement they can produce. This limitation, combined with the result of ref. 7, signals the end of passive linear optics as the universal testbed for quantum phenomena—most quantum states are not accessible using passive postselection.

2 Graph states from linear optics

We first introduce graph states, and local complementation, which generates each graph-state entanglement class.

Graph states are n-qubit stabiliser states which have a direct correspondence to undirected n-vertex (order n) graphs. A graph state, $|G\rangle$, corresponding to the graph $G=(V,E)$ with a set of vertices V, and a set of edges E, is written:

$$|G\rangle = \prod_{(i,j)\in E} \mathrm{CZ}_{ij} |+\rangle^{\otimes |V|} \tag{1}$$

Where $|+\rangle = (|0\rangle + |1\rangle)/\sqrt{2}$ and $\mathrm{CZ} = |00\rangle\langle 00| + |01\rangle\langle 01| +$

*josh.silverstone@bristol.ac.uk

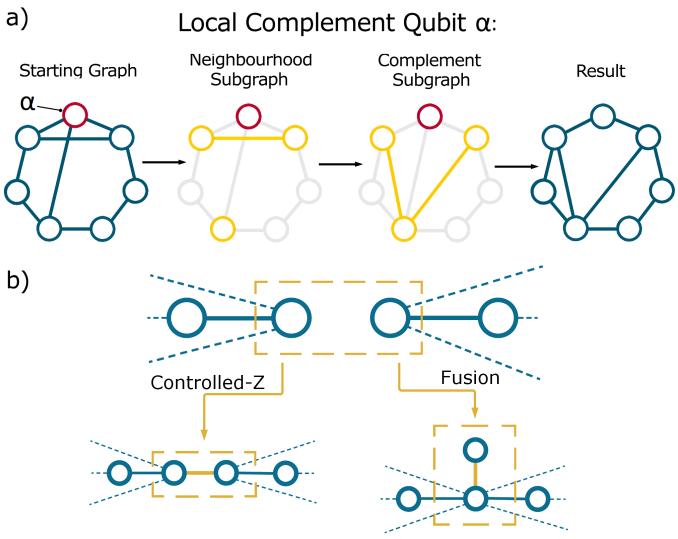

Figure 1: a) Local complementation of qubit α on a seven qubit graph state. The subgraph containing only the neighbours of α is complemented (if present, edges are removed, if not present, edges are added). b) CZ adds an edge to the graph. Fusion performs a vertex merge on the two qubits, and adds a vertex connected to the merged vertex [26]. Dashed edges represent any edge that might connect to the subgraph to its surroundings.

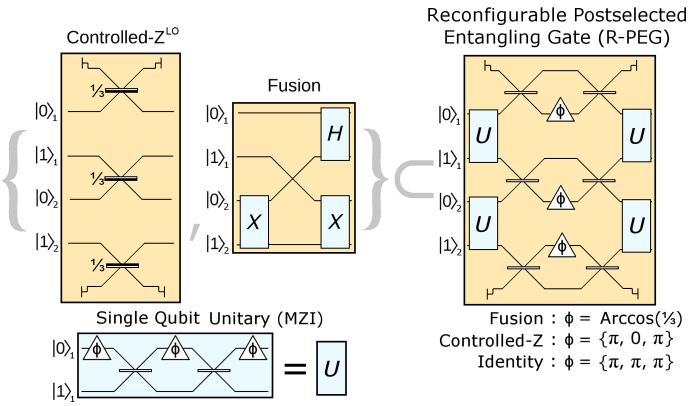

Figure 2: The two types of entangling gate discussed here: postselected fusion and postselected CZ^{LO}, as well as a MZI implementing a single qubit. Local operations can be implemented by the single qubit MZI (blue). The reconfigurable postselected entangling gate, (R-PEG), introduced here, can perform both gates as well as LCs, and so is the only gate needed to postselect graph states in linear optics. Unlabelled beamsplitters are 50:50 with a realistic (for integrated optics) i phase on reflection, the $\frac{1}{3}$ beamsplitters give a sign change on reflection from the light side.

$|10\rangle\langle 10| - |11\rangle\langle 11|$. Graph states are thus real, equal-weight states.

Graph states may be transformed using local operations into any stabiliser state [33], for example, star-type graph states are locally equivalent to GHZ states. Most states, however, are not locally equivalent to a graph.

2.1 Local complementation

Some graph states are equivalent under local unitary transformations. In the graph representation, graphs which can be transformed into one another by successive applications of local complementation (LC) are locally equivalent [34, 35]. On a graph, LC_α acts to complement the neighbourhood of some vertex α (see figure 1a). Specifically, successive application of the following local unitary, which implements LC_α on a graph G, can produce the entire set of states that are local unitary (LU) equivalent:

$$\mathrm{LC}_\alpha = \sqrt{-iX_\alpha} \bigotimes_{i \in N_G(\alpha)} \sqrt{iZ_i} \qquad (2)$$

where $\sqrt{-iX} = \frac{1}{\sqrt{2}}\left(\begin{smallmatrix} 1 & -i \\ -i & 1 \end{smallmatrix}\right)$ and $\sqrt{iZ} = e^{\frac{i\pi}{4}}\left(\begin{smallmatrix} 1 & 0 \\ 0 & i \end{smallmatrix}\right)$. In optics, these local operations are implemented experimentally with local Mach-Zehnder interferometers, (where the neighbourhood of qubit α, $N_G(\alpha)$, must be known). Here, we write $\mathrm{LC}_\alpha(|G\rangle)$, describing a unitary operation on quantum state $|G\rangle$, and $\mathrm{LC}_\alpha G$, the graph operation on graph G, interchangeably, $|\mathrm{LC}_\alpha(G)\rangle = \mathrm{LC}_\alpha|G\rangle$.

In graph-theoretic terms, local complementation realises, $\mathrm{LC}_\alpha(G(V,E)) :\to G(V,E'); E' = E \cup K_{N_G(\alpha)} - E \cap K_{N_G(\alpha)}$, for some graph $G(V,E)$. Here, $K_{N_G(\alpha)}$ is the set of edges of the complete graph on the vertex set $N_G(\alpha)$. Equally, the subgraph induced by the vertex set $N_G(\alpha)$, $G[N_G(\alpha)]$, is complemented (has its edges toggled), leaving the rest of G unchanged.

Any class of locally equivalent graph states can be generated using a starting member and repeated application of this operation, which is illustrated in Figure 1a. Refs. 34, 35 describe these and other useful properties of graph state entanglement. For a full treatment of single qubit operations on graph states, see refs. 36, 37.

2.2 Postselected entangling gates (PEGs)

A gate configuration is postselectable if and only if all possible gate failure combinations can be detected, and ignored—when the postselected success signal is observed, all gates have performed the desired operation.

We distinguish two types of entangling gate in used linear optics—postselected gates and heralded gates—both of which are probabilistic. If a gate is postselected, there are no auxiliary photons, and no photons are consumed by the gate. Heralded gates, on the other hand, either consume auxiliary photons as a resource (such as in the Knill-Laflamme-Milburn scheme [7]), or consume one or more of the input-state photons (such as the cannonical fusion gate [25]). In both cases, the measurement outcome "heralds" the result of the gate.

By use of measurement and feed-forward, heralded gates remove any non-qubit components of the state, whereas PEGs produce a state which contains terms outside of the qubit subspace, until all photons are finally measured. Note that heralded gates with feedforward are sufficient for universal quantum computation [7], whilst postselected gates are not. Here, we only consider postselected gates. To unstand transformations of Fock states without postselection, refer to ref. 38.

PEGs are interferometers which couple modes between qubit mode pairs, implementing the desired operation on the qubit subspace, $\mathcal{Q}$. Components of the state in the "junk" non-qubit subspace, $\mathcal{J}$, are discarded. Here, $\mathcal{J} = \mathcal{F} - \mathcal{Q}$, where $\mathcal{F}$ is the space of all Fock states with n or fewer photons, and $\mathcal{Q}$ is the qubit subspace, defined in the next paragraph. These gates

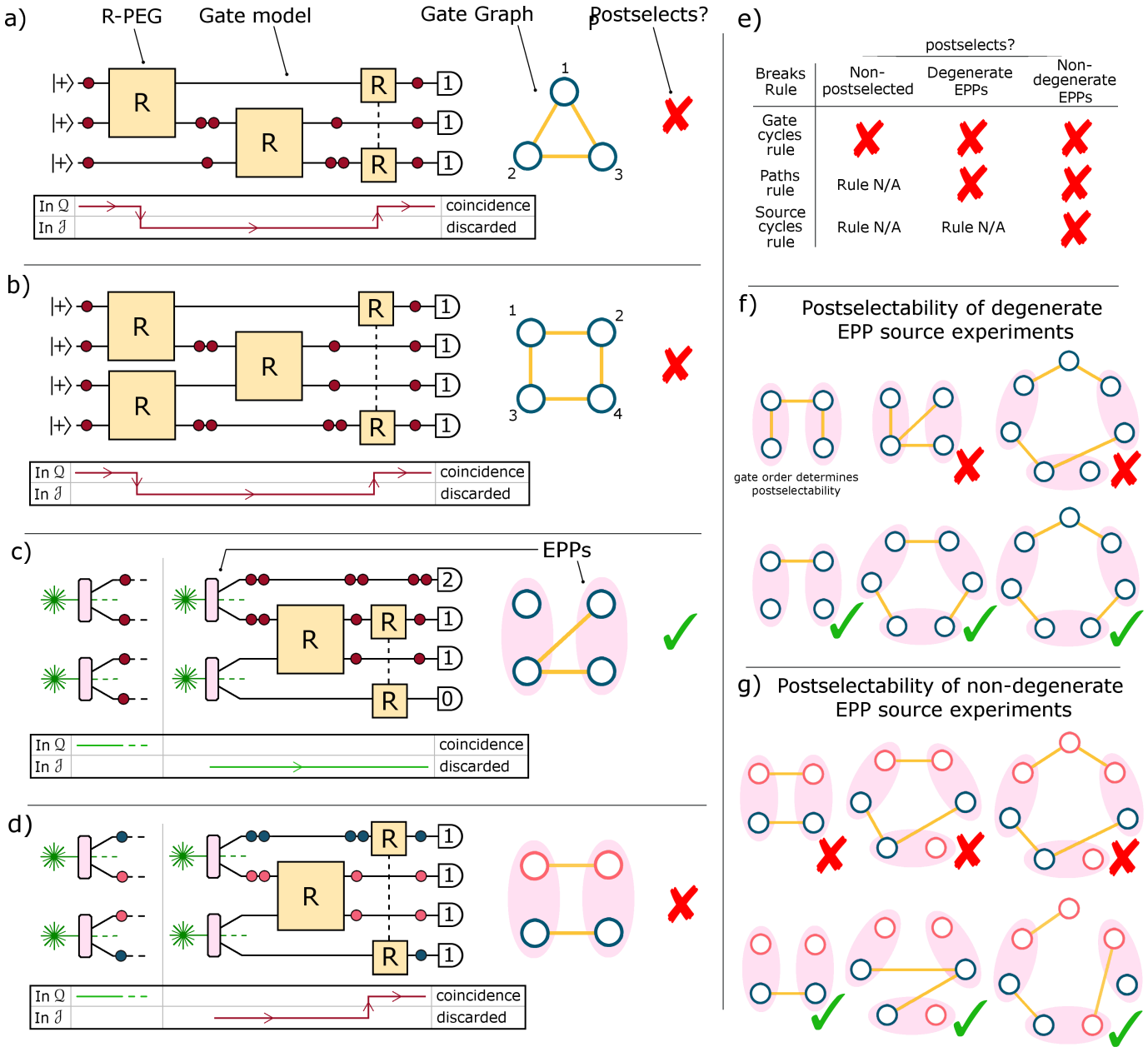

Figure 3: Source and gate arrangements and postselection. a) A single Fock state vector traverses a cyclic gate arrangement, getting placed back in the postselected qubit basis, $\mathcal{Q}$, by the final, cycle-inducing gate. We say the experiment does not postselect in this case, as gate failure is masked. b) Example of an experiment not postselecting that involves concurrent initial gates. Each initial gate produces photon-rich and photon-poor qubits which travel in opposite directions around the gate cycle, until the state re-enters $\mathcal{Q}$. c) A source term in $\mathcal{Q}$ is shown next to a source term in $\mathcal{J}$. Junk states from degenerate EPP sources can effect postselectability, however this example does postselect, as there is no path back to $\mathcal{Q}$. d) Junk states from non-degenerate EPP sources re-entering $\mathcal{Q}$. e) Table summarising postselection rules. The paths rule is specifies a necessary condition, whilst the gates cycles and sources cycles rules specify sufficient conditions. f) Elemental examples of postselectability from degenerate EPP sources. g) Elemental examples of postselectability from non-degenerate EPP sources. Note that all cases that do not postselect in the non-degenerate case do not postselect in the degenerate case. Here, all examples which do not postselect break the paths rule. Outside of the paths rule, the order of the gates can effect postselectability, but for most of these examples, it does not. For degenerate sources, there exist n-photon, $n/2$-gate experiments that postselect. In the non-degenerate case, at most $\lceil n/2 \rceil - 1$ gates can be used, since $n/2$ gates will produce cycles between the sources.

are probabilistic because some of the state remain outside of $\mathcal{Q}$

We consider the dual-rail encoding, where pairs of optical Fock modes (f) constitute a logical qubit, $|0\rangle_i \leftrightarrow |01\rangle_f$, $|1\rangle_i \leftrightarrow |10\rangle_f$. Then $\mathcal{Q}_i = \text{span}(\{|0\rangle_i, |1\rangle_i\})$ and $\mathcal{Q} = \bigotimes_i \mathcal{Q}_i$. To postselect, we project on to $\mathcal{Q}$ with projector $P_{\mathcal{Q}}$.

Here, we use the postselected CZ (success probability $1/9$) [23, 24], which we denote CZ^{LO}, and a postselected version of the fusion gate, F (success probability $1/2$) [25, 26]. These gates can both be implemented by the reconfigurable postselected entangling gate (R-PEG), shown in Figure 2. The R-PEG consists of three Mach-Zehnder interferometers (MZIs) over six modes. This interferometer is a powerful tool

in the design of experiments—graph state generator experiments can comprise only of R-PEG gates. We return to experiment design in Section 4.5.

Interferometers implement linear mode (Bogoliubov) transformations, which map Fock states to other Fock states unitarily. Here, CZ^{LO} and F are interferometers, and by using the dual-rail mapping between qubits and Fock modes, as well as postselection $P_{\mathcal{Q}}$, we can evaluate the effect of these interferometers on qubit states. To enforce that interferometer inputs be in $\mathcal{Q}$ we apply $P_{\mathcal{Q}}$ on the right-hand side. CZ^{LO} can be realised with the R-PEG by setting $\phi = \arccos(\frac{1}{3})$, yielding:

$$P_{\mathcal{Q}}\mathrm{CZ}^{LO}P_{\mathcal{Q}} = \frac{1}{3}\mathrm{CZ}$$

So $P_{\mathcal{Q}}\mathrm{CZ}^{LO}P_{\mathcal{Q}} = \mathrm{CZ}$ after renormalisation.

The postselected fusion gate, F, swaps $|1\rangle_1$ and $|1\rangle_2$ of its two input qubits, and applies a Hadamard gate to qubit 1 as shown in Figure 2a [18, 26, 39]. This non-unitary operation removes any $|01\rangle_{12}$ or $|10\rangle_{12}$ qubit components of the state by transforming them to two-photon-per-qubit components in $\mathcal{J}$, which are discarded by postselection $P_{\mathcal{Q}}$ (coincidence detection). Fusion may be written in the qubit basis as:

$$P_{\mathcal{Q}}FP_{\mathcal{Q}} = \frac{1}{\sqrt{2}}(|+0\rangle\langle 00| + |-1\rangle\langle 11|)$$

This is an entangling operation. For example, the action of this gate on the separable state $|{+}{+}\rangle$ results in the (subnormalised) entangled two-qubit graph state $P_{\mathcal{Q}}F|{+}{+}\rangle = \frac{1}{2}(|+0\rangle + |-1\rangle)$. See Figure 1b for the gate's action on a graph state.

3 The limits of postselection

In this section we will demonstrate why certain arrangements of gates are not postselectable, and derive a criterion for success. Further, we examine combinations of PEGs and EPP sources and develop simple criteria for their postselectability.

3.1 Criterion for gate postselectability

Which gate arrangements are postselectable? Convention holds that sequential PEGs may lead to gate failure masked as success (these combinations are not postselectable). Below, we derive a condition on the arrangement of these gates for postselectability.

We wish to understand when a given combination of gates is not postselectable. To do so, we analyse the evolution of junk states (in $\mathcal{J}$) produced by PEGs. Since coincidence detection ensures that we only count output states with one photon in every qubit, we disregard parts of $\mathcal{J}$ with fewer than n photons (for n qubits in $2n$ modes). Here, we use "qubit" to refer to a pair of modes, whether they are occupied by photons, or not.

First, we discuss some properties of PEGs. When a gate fails, it produces an output state in $\mathcal{J}$, resulting in a qubit with no photons, and another with excess photons—one is photon-poor, and the other is photon-rich. Gates can also move states from $\mathcal{J}$ back into $\mathcal{Q}$. They can redistribute photons so that different qubits become photon-poor and photon-rich, throughout the circuit. If an arrangement of gates can move the state out

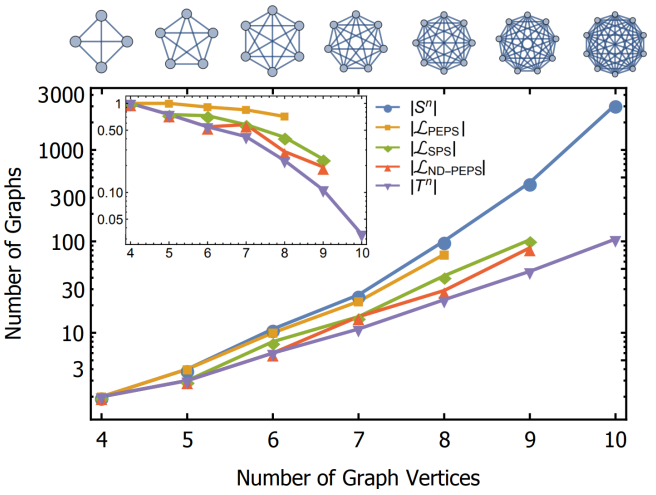

Figure 4: Logarithmic plot of the number of graph state entanglement classes accessible to different resource states with n qubits, $|\mathcal{L}_R|$, as well as the total number of classes, S^n, and the number of trees with n vertices T^n. Here $\mathcal{L}_{\mathrm{EPP}}$ is the set of classes accessible to degenerate entangled postselected pairs, $\mathcal{L}_{\mathrm{SPS}}$ is the set of classes accessible to heralded single photon sources, and $\mathcal{L}_{\text{ND-EPP}}$ is the set of classes accessible to non-degenerate entangled postselected pairs. Inset: number of postselectable classes as a proportion of the number of entanglement classes. Isomorphic graphs are counted only once. Sequences from [40, 41].

of the qubit basis, $\mathcal{Q}$, and subsequently return to it, we say the gate arrangement is not postselectable, as the gate failure is masked (see Figure 3a-b). Equally, the information of whether a the gate succeeded or failed is erased.

To re-enter $\mathcal{Q}$, the photon-poor and photon-rich qubits must meet again—after being generated together—by taking different paths through the experiment. Together, their paths form a loop. If we draw the gate configuration as a graph (with vertices as qubits, and edges as gates), then this loop corresponds to a cycle in that graph. Such a cycle is the only way the state can leave and subsequently re-enter $\mathcal{Q}$. Thus, configurations with cycles are not postselectable.

This holds for any time-ordering of the gates. In a cycle of gates, each gate's output is connected to an input of another gate. Junk is produced by all of the first time-step gates, re-entering $\mathcal{Q}$ by the the subsequent gates that link them. An example is shown in Figure 3b.

Therefore, a sufficient condition for successful gate postselection can be stated succinctly as *Experiments containing cycles of PEGs are not postselectable*. We will refer to this as the "gate cycles rule".

For example, attempting to produce a three qubit "triangle" graph state using three postselected CZ^{LO} gates applied to $|{+}{+}{+}\rangle$ will not be successful:

$$\begin{aligned}|\psi\rangle = &\ P_{\mathcal{Q}}\,CZ_{31}^{LO}\,CZ_{23}^{LO}\,CZ_{12}^{LO}\,|{+}{+}{+}\rangle \\ &= \frac{1}{108}\left(\sqrt{2}+4\sqrt{3}\right)|000\rangle \\ &+ \frac{1}{54\sqrt{2}}\left(|001\rangle+|010\rangle-|011\rangle+|100\rangle-|101\rangle-|110\rangle\right) \\ &+ \frac{1}{324}\left(4\sqrt{3}-3\sqrt{2}\right)|111\rangle\end{aligned}$$

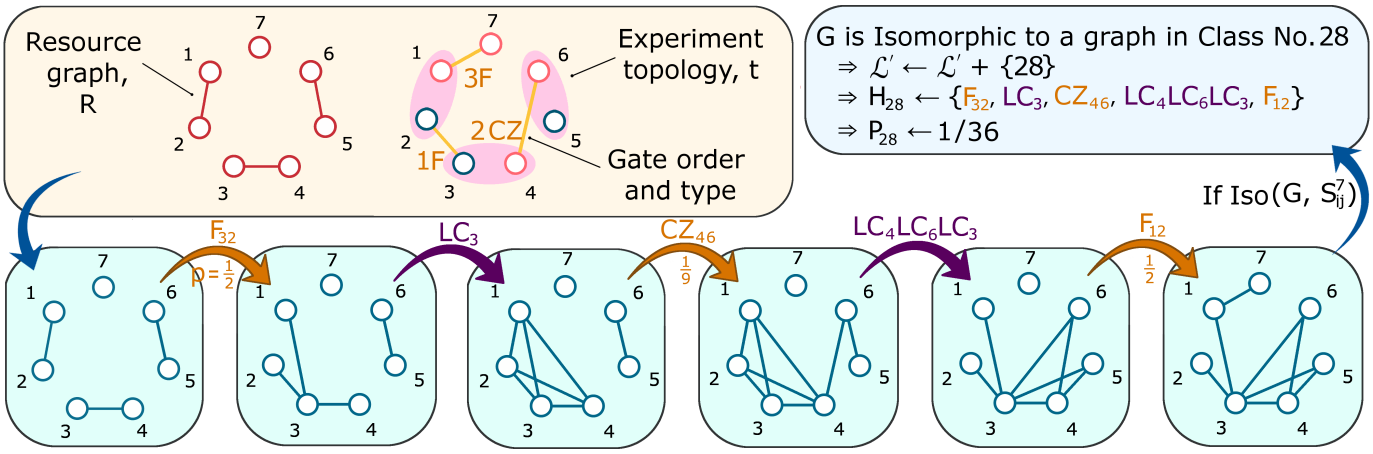

Figure 5: An example of one Monte Carlo iteration of FINDACCESSIBLECLASSES. Starting from a given resource state, in this case three non-degenerate EPPs and a heralded single photon, operations for an entangling strategy are performed in order, interspersed with LCs on the previously acted upon vertices. If the resulting graph is not isomorphic to any graph found thus far, the entanglement class of the graph i is saved to a set $\mathcal{L}'_R$. After many runs, $\mathcal{L}'_R \approx \mathcal{L}_R$. An alternate example can be found in supplementary material 1.2.

$|\psi\rangle$ differs significantly from the desired state, which has equal weights of $1/(3\sqrt{2})$ with signs $\{+,+,+,-,+,-,-,-\}$. This is because junk terms produced by the first gate is placed back in to the postselected basis by the subsequent gates. The squared amplitude of this postselected state is well above the expected success probability: $|\psi|^2 \approx 0.00706 > (\frac{1}{9})^3 \approx 0.00137$; the state is dominated by terms which have re-entered $\mathcal{Q}$, scrambling the state. Cycles of fusion similarly scramble the state, resulting in states which are dominated by junk components re-entering $\mathcal{Q}$.

We note that in reference [26] the authors claim that any graph state can be produced using postselected fusion only (with a focus on 2d lattice states). We can now see this claim to be unwarranted, since the scheme violates the gate cycles rule.

We are unaware of any PEG that does not lead to two-photon-per-qubit terms, and indeed, such a gate would require there to be no photonic path between the modes of its input qubits. Such a gate will be postselectable even when used in cycles. To our knowledge, LCs, postselected CZ and postselected fusion represent the known capability of postselective linear optics' to produce graphs states—all two-qubit Clifford gates can be decomposed in a CZ with LCs [33].

3.2 Combining degenerate entangled postselected pair (EPP) sources with postselected gates

Ensembles of m EPP sources produce states mostly contained in $\mathcal{J}$, even in the $2m$-photon subspace (for $2m = n > 2$ qubits). This is because m coherently pumped sources produce a superposition of all permutations of m pairs produced in m sources (at the $2m$ photon level). Only one of these terms is in $\mathcal{Q}$—the term where one pair is produced in each source—the rest are in $\mathcal{J}$ (see Supplementary Material 1.5). Because of this, gate arrangements may not be postselectable even in the absence of cycles, if they take EPPs as input, since the input superposition already contains junk. Hence this scenario requires postselectability criteria more strict than the gate cycles rule alone.

The most numerous form of junk state produced by an ensemble of m pair sources is one with two photon-rich qubits (from source i) and and two photon-poor qubits (from source $j \neq i$). Gates that disjointly connect the qubits from source i to the qubits from source j will always mask gate failure because of such terms. By disjointly, we mean that the two paths do not share gates (edges), however they may share vertices. The excess photons from source i can travel via gates to the qubits from source j and hence re-enter $\mathcal{Q}$, and hence are not postselectable. This is depicted as "gate arrangement graphs" in Figure 3d. Unpostselectable examples are shown in Figure 3d,f,g.

Hence *Experiments containing a pair of disjoint paths in the gate arrangement graph that connect the qubits from one EPP source with the qubits from another, are not postselectable*. We will call this the "paths rule". In this case, because each gate acts independently—simply moving a photon toward the photon-poor qubit—the experiment does not postselect no matter which the order of gates are applied in.

The paths rule only accounts for superposition components where one EPP source fired twice, and one did not fire at all. Some gate configurations, however, are not postselectable only because of junk produced by more than two sources. The paths rule is a necessary, but not sufficient, condition of postselectability in these circumstances: i.e. an experiment which satisfies the paths rule may still be unpostselectable. Due to the combinatorial number of gate and source permutations, a sufficient condition for postselectability of combinations of PEGs and degenerate EPP sources is not forthcoming. In section 4, we apply numerical methods to evaluate postselectability, determining which graph states are postselectable from combinations of PEGs and EPP sources.

3.3 Non-degenerate nonlinear sources and postselected gates

An interesting and commonly used class of EPP source are those with non-degenerate photons, that is, photons of different colours, polarisations, etc. Since pairs of input pho-

tons are distinguishable, an experiment will typically put them through separate sets of gates. Though all interferometers that are not postselectable in the non-degenerate are also not postselectable in the degenerate case, the total number viable gate topologies with non-degenerate sources is drastically reduced,

For non-degenerate EPPs, combining this restriction with the paths rule implies that cycles made between the different sources *sufficiently* determines postselectability.

To see this, we examine experiments of m non-degenerate EPP sources. Take two sources i and j emitting "red" and "blue" photons. If the red-photon qubits from both sources are connected via gates, then the only way to form a cycle between the sources is to connect the corresponding blue-photon qubits, which would close a second path between i and j and so would violate the paths rule. Hence, *in experiments of non-degenerate EPP sources, cyclic combinations of sources and gates are note postselectable*. We will call this combined rule the "source cycles rule".

What about other terms in the superposition of Fock states produced by the source, such as when three pairs are produced in one source and none are produced in two others? We will show that the source cycles rule is a sufficient condition for postselectability

In a $2m$-photon, m-source experiment, we examine the case where one of the sources fired m times. Here, to re-enter the postselected basis,$\mathbb{Q}$, at least $2(m-1)$ gates must be used (each photon-poor qubit must be addressed at least once). However, the sources cycles rule is a more stringent than this—a cycle is formed between sources with just $m-1$ gates (an intrinsic property of tree graphs). Since any source term where sources fire $p < m$ times are a subcases of the above, the source cycles rule is *sufficient* for determining postselectability of non-degenerate EPP source experiments.

4 Which graph states are postselectable?

Now that we are familiar with the rules of postselecting graph states, we can establish which states can be accessed, and which states cannot.

First, we lower bound the number of classes that are accessible from the popular resource state of n non-degenerate pair sources, with the number of trees (non-cyclic graphs). This follows from the fact that trees can always be constructed from this resource (see Supplementary Material 1.1), and that there is at most one tree in each entanglement class [42]. Figure 4 compares the number of trees to the number of entanglement classes for increasing qubit (vertex) number, and reveals a super-exponential divergence [40, 41, 43].

Because of the combinatoral number of possible experiments using PEGs and LCs, we turn to numerical methods to discover exactly which classes of entanglement are accessible to postselective linear optics given a certain resource state. Our approach is to sample allowed combinations of entangling gates and local complementations, and catalogue the graph states which result. By using the LCs, postselected CZ and fusion gates, we span the currently known capability of postselective linear optics' to produce graphs states; though gates can only be applied in trees, the use of LCs allows access to a wider variety of graph state classes—including those not containing trees. Note that all two-qubit Clifford gates can be decomposed into a CZ with LCs [33]. We use the canonical indexing provided by Hein, Cabello, *et al.* in refs. 30, 34. We denote the set of graph state class indices that can be accessed by a given resource state R by $\mathcal{L}_R$.

4.1 Numerical Methods

In [30, 40], tables of representative members for each entanglement class up to $n = 12$ are provided. Starting from these supplied graphs, we take random walks to explore each LU class (which are of known size). We denote the j^{th} n-vertex graph of entanglement class i as S^n_{ij}, where S^n_i is the set of all graphs in that entanglement class and S^n is the set of all n-vertex classes, $S^n = \cup_i S^n_i$. Note $S^n_a \cap S^n_b \neq \emptyset \quad \forall a, b$.

We explore which graph states are accessible to linear optics and PEGs with our algorithm FINDACCESSIBLECLASSES (visually depicted in Figure 5 and provided in Supplementary Material 1.2). This algorithm enumerates accessible entanglement classes for a given resource state R, and stores the list of accessible classes as $\mathcal{L}'_R \approx \mathcal{L}_R$. The results of our investigation using FINDACCESSIBLECLASSES are shown in Table 1. To aid the classification of any newly found graphs, S^n is stored in memory. We provide plain-text and Mathematica representations of S^n, up to $n = 9$ qubits, as well as a Mathematica implementation of FINDACCESSIBLECLASSES. These can be found in the Supplementary Material [44].

Each iteration of FINDACCESSIBLECLASSES starts with a resource graph state R, and a randomly chosen n-qubit experiment satisfying out postselection rules. This n-vertex gate arrangement is a graph, t, which corresponds to a linear optical experiment composed of PEGs. t is generated randomly from a set T, which depends on the resource (see Section 4.2). Each edge of t is randomly assigned either a CZ or an F gate, and a random time ordering. Random combinations of relevant LCs are interspersed between gates (see section 4.3), to increase the variety of accessible graphs. As the quantum operations are compactly represented as operations on graphs, we can avoid the exponential memory requirement of simulating quantum states. This Monte-Carlo approach is designed to fairly sample the graph-state generation experiments available to postselected linear optics, by using LCs, postselected CZ and fusion gates.

After all specified entangling operations have been performed, we store the entanglement class that has been reached, in $\mathcal{L}'_R$. We store the gates and local complementations used, in H^R. Thus, H^R_i is the *recipe* for accessing entanglement class i with resource state R. These recipes are overwritten when a more efficient one is found. We keep sampling, until no more novel classes are found, at which point we assume we have sampled them all: $\mathcal{L}'_R \approx \mathcal{L}_R$.

4.2 Resource States

To fairly sample from postselectable experiments, the sets of allowed gate arrangements, T, varies for the different classes of resource: heralded states, degenerate EPPs and non-degenerate EPPs. In all cases, relevant LCs are interspersed between the gates.

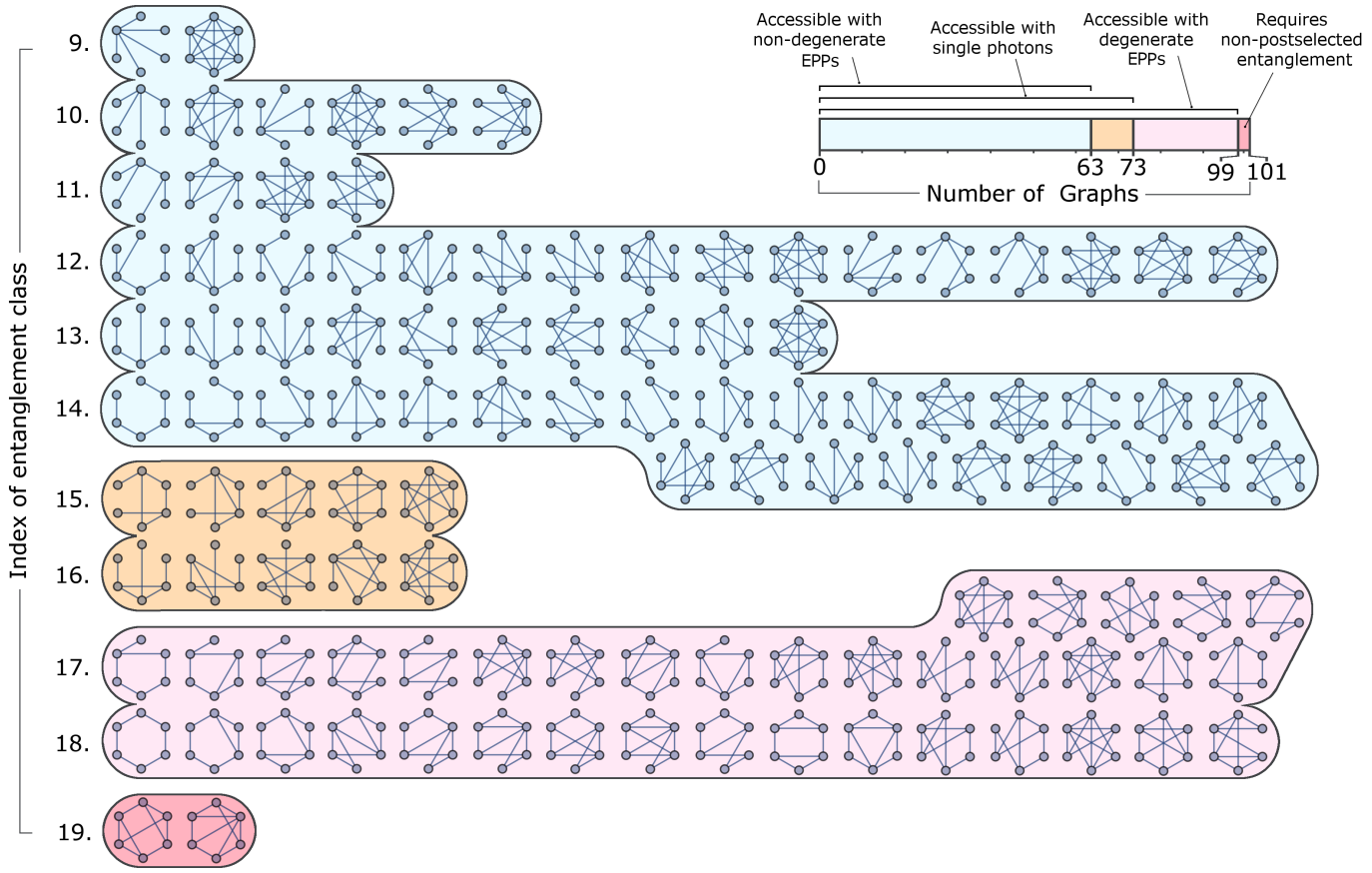

Figure 6: Six photon graph states organised in to their LU classes, cannonically indexed starting from the 2-vertex graph state. See Supplementary Material 1.3 for a complete list of graph states indexed up to 8 vertices. A resource of non-degenerate postselected pairs can access all of the graphs shown in blue, whilst a resource of single photons can access all of the states shown in orange and blue, and a resource of degenerate postselected pairs can access all of the graphs shown in pink, orange and blue. Graphs shown in red require a heralded entangled resource state to be produced using PEGs.

For a heralded resource (one not involving postselected sources), our algorithm must sample from all possible experiments that do not contain a cycle of PEGs. Hence T is the set of all connected trees with n vertices. There are $2^{n-1}n^{n-2}(n-1)!$ such experiments. This is the number of labelled trees [45] multiplied by both the number of possible edge labellings $\{\mathrm{CZ},\mathrm{F}\}$ and the number of gate orderings. Labelled trees are fairly sampled by the Pruefer sequence method [46]. We sample from the set of all isomorphisms (labellings) of every tree, as to consider only one labelling of the resource state.

For a heralded resource that has some entanglement, not all of the gates represented by $t \in T$ need be applied to obtain n-partite entanglement. In FINDACCESSIBLECLASSES, the number of gates applied are chosen at random, where the minimum number of gates could still feasibly output an n-qubit connected graph. For example starting with 3 heralded entangled pairs, only two gates are needed to produce a 6-qubit state, however more entanglement classes are accessible by using up to 5 gates. Hence, we randomise over the different number of gates. An example member of $t \in T$ is shown in Figure 5, with its ordered edge-labelling. The set of trial gate arrangement trees, T, can also be tailored to encode any restriction in gate topology, for example where only nearest-neighbour gates are permitted.

Non-degenerate EPPs require $m-1$ gates to be globally entangled—and are not postselectable with m gates, as a cycle will form between sources. In this case, the number of gates is fixed, and we only sample over the trees of order m. Since $m = n/2$, and the number of trees scales exponentially with n, the search space for non-degenerate pairs is drastically smaller than for any other input resource.

In the case of a resource state of degenerate EPPs, postselectability of a particular gate arrangement must be evaluated more directly, since we have no sufficient postselection rule rely on in this case. We evaluate random (non-interacting) photon scattering through the gate arrangement, for each source term in $\mathcal{J}$. If the photons can return to a one-per-qubit state, in $\mathcal{Q}$, then the gate combination is discarded, as it is unpostselectable. Although this method is not exhaustive, a sufficiently large number of iterations can guarantee accuracy. Due to the extra cost associated with this subroutine, FINDACCESSIBLECLASSES evaluates the postselectability of one experiment, then permutes the choice of gate (CZ or F), as well as the LCs applied, for 50 experiments which share the topology. This greatly increases the efficiency of class discovery, and is analogous to finding the classes accessible by a single linear optics experiment which utilises the reconfigurable PEG of Figure 2.

n	Resource state, R	Indices of LU classes accessed, $\mathcal{L}'_R$	$\lvert\mathcal{L}'_R\rvert/\lvert S^n\rvert$
4	2 non-degenerate EPPs	3, 4	$2/2=1$
5	2 non-degenerate EPPs & 1 single photon	5 to 8	$3/4=0.75$
5	5 single photons	5 to 8	$3/4=0.75$
5	2 degenerate EPPs & 1 single photon	5 to 9	$4/4=1$
6	3 non-degenerate EPPs	9 to 14	$6/11\approx 0.54$
6	6 single photons	9 to 16	$8/11\approx 0.73$
6	3 degenerate EPPs	9 to 18	$10/11\approx 0.91$
6	2 pairs & 2 single photons	9 to 19	$11/11=1$
7	3 non-degenerate EPPs and 1 single photon	20 to 32, 34, 36	$15/26\approx 0.58$
7	7 single photons	20 to 32, 34, 36	$15/26\approx 0.58$
7	1 pair and 5 single photons	20 to 41	$22/26\approx 0.85$
7	3 degenerate EPPs & one single photon	20 to 41	$22/26\approx 0.85$
7	2 entangled pairs & 3 single photons	20 to 45	$26/26=1$
8	4 non-degenerate EPPs	46 to 68, 70, 73, 74, 79, 89, 92	$29/101\approx 0.29$
8	8 single photons	46 to 79, 83, 86 to 87, 89, 92, 94, 104, 107, 121, 143	$42/101\approx 0.42$
8	1 pair & 6 Single Photons	46 to 108, 114, 115, 117, 121, 123 to 125	$73/101\approx 0.72$
8	4 degenerate EPPs	46 to 68, 70, 75, 76, 78 to 80, 82, 83, 86 to 89, 92 to 98, 100, 101, 103, 108, 109, 110, 112 to 116, 118 to 121, 123 to 125, 127, 129, 130, 133, 134, 136, 139, 141, 144, 145	$72/101=0.71$
8	4 entangled pairs	46 to 140, 142 to 144, 146	$99/101\approx 0.98$

Table 1: Which classes of graph state can be generated using PEGs given different resource states R, written $\mathcal{L}'_R$. These classes (denoted S^n_i) are indexed starting from the 2-vertex graph state. See Supplementary Material 1.3 for a complete list of graph states indexed up to 8 vertices (from refs. [30, 34, 40]). Results for $n=9$ can be found in supplementary material 1.3. This table was generated by FINDACCESSIBLECLASSES.

4.3 Sampling linear optical graph experiments

Applying local operations between gates can yield a wider variety of accessible graph states. Just a few LC operations are sufficient. After a CZ_{ij} operation, LCs need only be applied to qubits i and j, since CZ commutes with LC in all other cases. After a F_{ij} operation, LCs need only be applied to qubits in $\{N_G(i)\cup N_G(j)+\{i\}+\{j\}\}$, for the same reason, where $N_G(i)$ is the graph neighbourhood of vertex and qubit i. Furthermore, ≤ 5 randomly chosen LC operations are needed after a CZ gate, since LC around two vertices is periodic with period 6 [47]. Similarly, ≤ 14 LCs are needed after a fusion, as this is the largest number of LC operations needed to traverse the widest class for $n\leq 9$ qubits (from numerics). Higher qubit numbers will require concomitantly larger numbers of post-fusion LCs. Proofs are shown in Supplementary Material 1.1.

The size of the configuration space for a resource of heralded single photons is $O(2^{n-1}d_n^{n-2}n^{n-2}(n-1)!)$, where d_n is the diameter of the orbit of the largest n-qubit entanglement classes ($d_9=14$). For $n=8$ qubits the size of this configuration space is $\approx 1.3\times 10^{18}$; for $n=10$ it explodes to $\approx 2.7\times 10^{25}$. This makes an exhaustive search impossible, and motivates our use of sampling methods.

Each newly found n-vertex graph, G, is likely to be isomorphic, not identical, to the corresponding graph in the stored database of entanglement classes, S^n. Consequently, GRAPHISOMORPHISM, which is computationally hard, must be computed for a range of graphs so that the candidate graph can be properly catalogued. For small numbers of vertices, however, the problem is tractable.

4.4 Which classes are accessible?

We have enumerated the entanglement classes that are accessible using certain resource states and PEGs. The results are shown in Table 1. Interestingly, those states which are inaccessible tend to have higher canonical indices, ordered both by vertex degree, and by the minimum number of edges on a graph in the class. This also correlates with known bounds on the Schmidt rank [30, 34].

Without exploring the entire space, there is no guarantee that all classes have been found, however FINDACCESSIBLECLASSES appears to converge after sampling a minuscule fraction of configurations. For the results in Table 1, the algorithm was terminated when no new classes were found in the last 5/6 of the total number of iterations. For the 8-qubit graphs, this corresponds to sampling about one in every 10^5 possible configurations.

Our exploration using $n\leq 9$ was performed using the (uncompiled, single-threaded) Mathematica implementation, on a standard desktop PC. We anticipate that, by using parallel, compiled code, up to $n=12$ vertex graphs can be investigated.

4.5 Designing graph state generators

Efficient experimental generation of graph states using photonics is a challenge. FINDACCESSIBLECLASSES can also be used for experiment design: to find a recipe which produces the desired graph state in class i. Repeat FINDACCESSIBLECLASSES with a reasonable resource state input R, maximising the probability of generation, P_i^R, and recording the recipe, H_i^R. Modify R until a satisfactory experiment is found: decrease P_i^R by using a more practical R or increase it (especially in the case where no graphs in i are found) by using a more entangled R. The recipe H_i^R yields the experiment which produces a graph in the target class i. We can use the R-PEG to realise each PEG (see Figure 2), where the single-qubit interferometers can perform the necessary local complementations. The optical depth of such circuits is $O(n)$ for n qubits.

Conversely, FINDACCESSIBLECLASSES can enumerate the graph states that a given interferometer can access, by fixing t and searching over different combinations of LC and gate type. In this way, combining the rules of postselection, and FINDACCESSIBLECLASSES and the R-PEG allows new graph generating experiments to rapidly checked for feasibility, and designed with maximum versatility.

5 Conclusion

Postselection remains the current, go-to tool for generating entanglement between photons in linear optics. We have described a severe and previously undocumented limitation of this technique, in the context of heralded sources, degenerate and non-degenerate postselected pairs. We have tabulated which graph states can be accessed using linear optics and PEGs for $n \leq 9$, and demonstrated that the number of states available to postselected systems diminishes rapidly with increasing qubit number. We have provided algorithms to calculate which states are accessible for graphs up to $n = 12$, limited only by the availability of class catalogue data.

Postselectable graph states that can be produced from EPPs are of interest, with experiments with up to 12 photons possible in the near future [19]. Whilst we have not found an analytic condition on postselectability for the combined postselection of degenerate EPPs and PEGs, our numerics show that a wide variety of states are nonetheless available to this resource—the majority of classes are accessible for $n \leq 8$. This is encouraging news for near-term demonstrations of entanglement using linear optics. It implies that postselected sources and gates may still have some mileage before true single photon sources become a necessity.

Despite their widespread use, a vanishing fraction of graph states are accessible using non-degenerate postselected pairs, and these accessible states tend to have low Schmidt rank. With heralded single photons, many more LU classes become accessible, but this too is a diminishing fraction of the total, as qubit number increases. Degenerate postselected pairs allow access to a wider variety of states, but still a diminishing fraction of the total. The end of the road for postselected quantum optics is now in sight. Heralded or deterministic gates for photon-photon interactions are not just a route to increased efficiency, but they are a *necessity* if we are to access any appreciable fraction of multi-qubit entanglement classes using optics.

Several questions remain unanswered. Why are certain states accessible and others are not? Why does interspersed local complementation allow for the creation of a wider variety of states? What is the size of the space accessible to hybrid experiments, part postselected, part heralded? Can this reasoning be applied to hyper-entangled, or qudit photonic states?

The limits of postselection are indeed severe, but, with the tools and understanding developed here, planning quantum information experiments which reach these limits will be possible. Multi-photon experiments are often phrased in a measurement-based or state-preparation language, both of which are enlightened by this work, in the context of postselection. These methods will allow experimenters to produce states with the minimum resource, and with the most efficient optical recipe, expediting progress toward large-scale quantum computation, with optics and otherwise.

Acknowledgements

The authors would like to acknowledge Mercedes Gimeno-Segovia, Sam Pallister, Patrick M. Birchall Stasja Stanisic, Will McCutcheon, and Rafaele Santagati for fruitful discussion and motivation. This work was supported by the UK Engineering and Physical Sciences Research Council (EPSRC). JCA and SMS are supported by EPSRC grant EP/L015730/1. JWS is supported by EPSRC grant and EP/L024020/1.

References

[1] Stuart J Freedman and John F Clauser. "Experimental test of local hidden-variable theories". *Physical Review Letters* 28.14 (1972), p. 938.

[2] Demid V Sychev et al. "Enlargement of optical Schrödinger's cat states". *Nature Photonics* 11.6 (2017), pp. 379–382.

[3] Alberto Peruzzo et al. "A quantum delayed-choice experiment". *Science* 338.6107 (2012), pp. 634–637.

[4] Paul Kwiat et al. "Experimental Realization of Interaction-free Measurements". *Annals of the New York Academy of Sciences* 755.1 (1995), pp. 383–393.

[5] Alain Aspect, Philippe Grangier, and Gérard Roger. "Experimental realization of Einstein-Podolsky-Rosen-Bohm Gedankenexperiment: a new violation of Bell's inequalities". *Physical review letters* 49.2 (1982), p. 91.

[6] Dik Bouwmeester et al. "Observation of three-photon Greenberger-Horne-Zeilinger entanglement". *Physical Review Letters* 82.7 (1999), p. 1345.

[7] Emanuel Knill, Raymond Laflamme, and Gerald J Milburn. "A scheme for efficient quantum computation with linear optics". *Nature* 409.6816 (2001), pp. 46–52.

[8] Mercedes Gimeno-Segovia et al. "From three-photon Greenberger-Horne-Zeilinger states to ballistic universal quantum computation". *Physical review letters* 115.2 (2015), p. 020502.

[9] Sam Morley-Short et al. "Physical-depth architectural requirements for generating universal photonic cluster states". *Quantum Science and Technology* 3.1 (2017), p. 015005.

[10] Mihir Pant et al. "Percolation thresholds for photonic quantum computing". *arXiv preprint arXiv:1701.03775* (2017).

[11] Robert Raussendorf and Hans J Briegel. "A one-way quantum computer". *Physical Review Letters* 86.22 (2001), p. 5188.

[12] Joshua W Silverstone et al. "Silicon quantum photonics". *IEEE Journal of Selected Topics in Quantum Electronics* 22.6 (2016), pp. 390–402.

[13] Andrea Crespi et al. "Suppression law of quantum states in a 3D photonic fast Fourier transform chip". *Nature communications* 7 (2016), p. 10469.

[14] Jianwei Wang et al. "Multidimensional quantum entanglement with large-scale integrated optics". *Science* (2018), eaar7053.

[15] Jian-Wei Pan et al. "Experimental demonstration of four-photon entanglement and high-fidelity teleportation". *Physical Review Letters* 86.20 (2001), p. 4435.

[16] P. Walther et al. "Experimental one-way quantum computing". *Nature* 434 (2005), pp. 169–176.

[17] Chao-Yang Lu et al. "Experimental entanglement of six photons in graph states". *Nature Physics* 3.2 (2007), pp. 91–95.

[18] Xing-Can Yao et al. "Observation of eight-photon entanglement". *Nature photonics* 6.4 (2012), pp. 225–228.

[19] Xi-Lin Wang et al. "Experimental ten-photon entanglement". *Physical review letters* 117.21 (2016), p. 210502.

[20] Lynden K Shalm et al. "Strong loophole-free test of local realism". *Physical review letters* 115.25 (2015), p. 250402.

[21] Marissa Giustina et al. "Significant-loophole-free test of Bell's theorem with entangled photons". *Physical review letters* 115.25 (2015), p. 250401.

[22] CK Hong, Zhe-Yu Ou, and Leonard Mandel. "Measurement of subpicosecond time intervals between two photons by interference". *Physical review letters* 59.18 (1987), p. 2044.

[23] Holger F Hofmann and Shigeki Takeuchi. "Quantum phase gate for photonic qubits using only beam splitters and postselection". *Physical Review A* 66.2 (2002), p. 024308.

[24] TC Ralph et al. "Linear optical controlled-NOT gate in the coincidence basis". *Physical Review A* 65.6 (2002), p. 062324.

[25] Daniel E Browne and Terry Rudolph. "Resource-efficient linear optical quantum computation". *Physical Review Letters* 95.1 (2005), p. 010501.

[26] TP Bodiya and L-M Duan. "Scalable generation of graph-state entanglement through realistic linear optics". *Physical review letters* 97.14 (2006), p. 143601.

[27] Qing Lin and Bing He. "Weaving independently generated photons into an arbitrary graph state". *Physical Review A* 84.6 (2011), p. 062312.

[28] Ying Li et al. "Resource costs for fault-tolerant linear optical quantum computing". *Physical Review X* 5.4 (2015), p. 041007.

[29] Mehdi Mhalla and Simon Perdrix. "Complexity of graph state preparation". *arXiv preprint quant-ph/0412071* (2004).

[30] Adán Cabello et al. "Optimal preparation of graph states". *Physical Review A* 83.4 (2011), p. 042314.

[31] Mario Krenn, Xuemei Gu, and Anton Zeilinger. "Quantum experiments and graphs: Multiparty states as coherent superpositions of perfect matchings". *Physical review letters* 119.24 (2017), p. 240403.

[32] Xuemei Gu et al. "Quantum Experiments and Graphs II: Computation and State Generation with Probabilistic Sources and Linear Optics". *arXiv preprint arXiv:1803.10736* (2018).

[33] Simon Anders and Hans J Briegel. "Fast simulation of stabilizer circuits using a graph-state representation". *Physical Review A* 73.2 (2006), p. 022334.

[34] Marc Hein, Jens Eisert, and Hans J. Briegel. "Multiparty entanglement in graph states". *Physical Review A* 69.6 (2004), p. 062311.

[35] Maarten Van den Nest, Jeroen Dehaene, and Bart De Moor. "Graphical description of the action of local Clifford transformations on graph states". *Physical Review A* 69.2 (2004), p. 022316.

[36] Axel Dahlberg, Jonas Helsen, and Stephanie Wehner. "How to transform graph states using single-qubit operations: computational complexity and algorithms". *arXiv preprint arXiv:1805.05306* (2018).

[37] Axel Dahlberg and Stephanie Wehner. "Transforming graph states using single-qubit operations". *arXiv preprint arXiv:1805.05305* (2018).

[38] Piotr Migdał et al. "Multiphoton states related via linear optics". *Physical Review A* 89.6 (2014), p. 062329.

[39] B Bell et al. "Experimental characterization of photonic fusion using fiber sources". *New Journal of Physics* 14.2 (2012), p. 023021.

[40] Lars Eirik Danielsen and Matthew G Parker. "On the classification of all self-dual additive codes over GF (4) of length up to 12". *Journal of Combinatorial Theory, Series A* 113.7 (2006), pp. 1351–1367.

[41] *The On-Line Encyclopedia of Integer Sequences*. 2015. URL: `https://oeis.org/A000055`.

[42] André Bouchet. "Transforming trees by successive local complementations". *Journal of Graph Theory* 12.2 (1988), pp. 195–207.

[43] François Bergeron, Gilbert Labelle, and Pierre Leroux. *Combinatorial species and tree-like structures*. 67. Cambridge University Press, 1998.

[44] *Supplementary material*. 2018. URL: `https://github.com/ja0877/postselect_graphs`.

[45] Arthur Cayley. "A theorem on trees". *Quartery Journal of Mathematics* 23 (1889), pp. 376–378.

[46] H Prufer. "Neuer beweis eines satzes uber per mutationen". *Archiv derMathematik und Physik* 27 (1918), pp. 742–744.

[47] Lars Eirik Danielsen and Matthew G Parker. "Edge local complementation and equivalence of binary linear codes". *Designs, Codes and Cryptography* 49.1-3 (2008), pp. 161–170.

Supplementary Material

1.1 Proofs

Lemma 1. *All of the n-vertex graph states that are locally equivalent to a tree can be constructed from $\lceil \frac{n}{2} \rceil$ entangled postselected pairs (from postselected nonlinear pair sources) using only postselected CZ and fusion gates.*

Proof. The two distinct trees with $n = 4$ vertices (the "star" and "line" graphs) correspond to performing CZ^{LO} or fusion on two pairs respectively, which establishes the base case. The induction step is to show for any order $n+2$ tree, t, one can always find a feature of the tree that implies it could have been constructed from some order n tree, and the two vertex connected graph (entangled pair), using an egde-add (CZ) or fusion operation.

These features of t are as follows:

Feature 1: t has two vertices in a line formation, where the second vertex is only adjacent to the first. This corresponds to a CZ (edge-add) of an order n tree with the complete two-qubit graph.

Feature 2: Two leafs (vertices of degree 1) are adjacent to the same vertex of t (but no others). This corresponds to a fusion of an order n tree with the complete two-qubit graph.

To show that all trees have one of these Features, we perform another induction. All order $n+1$ trees can be constructed by adding a vertex (with connecting edge) to some n-vertex tree. We will show that these Features can disappear when adding a connected vertex, but only by creating the other Feature. Hence all trees have at least one of these features.

Feature 1 will disappear if a new vertex is connected to the degree-two vertex of the Feature. In this case, the new graph has Feature 2. Similarly, Feature 2 will disappear if a new vertex is connected to one of the vertices of Feature 1. This forms Feature 1. The only tree of three vertices has both of these features. Hence all trees have one of these two features.

Since all $n+2$ trees have one of these features, it is always possible to find a tree of order n that can be used to construct a tree of order $n+2$, down to $n = 4$ where we know how to make both of the trees.

Since each additional pair of vertices has only one gate acting on it, the postselection rules are not violated.

This completes the proof.

□

Lemma 2. $[CZ_{ij}, LC_\alpha] = 0 \; \forall \; \alpha \notin \{i, j\}$. *($CZ_{ij}$ commutes with LC applied to qubit α, LC_α when α is not one of the qubits acted upon by the CZ.)*

Proof. If $i, j \notin N_G(\alpha)$ the unitaries (graph operations) act on different qubits (vertices) and therefore commute. We now examine $i, j \in N_G(\alpha)$. Note that complementation of a subgraph defined by a fixed set of vertices commutes with a CZ operation, since both toggle the edges present in the graph (addition modulo 2). This can also be understood by examining the CZ and LC unitaries. In LC_α for $i, j \in N(\alpha)$, qubits i and j undergo a $\sqrt{iZ}$ operation, which is diagonal. Since CZ is also diagonal, these operations commute, that is $[\mathrm{CZ}_{ij}, \sqrt{iZ_k}] = 0$ for $k = i, j$. Note that $\sqrt{iZ_k} \otimes \sqrt{iZ_l}$ is also diagonal. Since $N_G(\alpha)$, is unaffected by the CZ, LC_α and CZ commute if $i, j \notin N(\alpha)$.

□

Lemma 3. *Repeated LC on i and j on some graph G has just one periodic path through the members of the LC class.*

Proof. This is demonstrated independently in terms of edge-local complementation in [47], but we provide an alternate proof. Since $\mathrm{LC}_\alpha \circ \mathrm{LC}_\alpha = \mathbb{1}$ there are only two ways uniquely apply LCs—alternating LC on i and j, i.e. $\ldots \mathrm{LC}_i \circ \circ \mathrm{LC}_j$ and $\ldots \mathrm{LC}_i \circ \mathrm{LC}_L \mathrm{C}_j$. This defines two paths through the members of the LC class.

We will now show these paths are periodic. In the following we denote the k^{th} LC operation of one of these trajectories as, LC^k,

Since there are a finite number of graphs equivalent under LC, alternating LCs must reproduce the initial graph, or the path will end after $k-1$ LCs, i.e. when some graph is reached whereby LC has no effect. In this case, $\mathrm{LC}^k = \mathbb{1}$ and the series of LCs can be written $\ldots \mathrm{LC}_i^{k+1} \circ \mathrm{LC}_j^k \circ \mathrm{LC}_i^{k-1} \circ \ldots \circ \mathrm{LC}_j^1 = \ldots \mathrm{LC}_i^{k+1} \circ \mathrm{LC}_i^{k-1} \circ \ldots \circ \mathrm{LC}_j^1$. Since $\mathrm{LC}_i \circ \mathrm{LC}_i = \mathbb{1}$, all LCs can be paired around LC^k and cancelled, leaving the identity, i.e. the operation is periodic with period $2k-1$.

We will now show that these orbits are the inverse of one another. Take one of the two orbits (say the one that starts with j) and assume it has period p, then $\mathrm{LC}_i^p \circ \mathrm{LC}_j^{p-1} \circ \ldots \circ \mathrm{LC}_j^1 (G) = G$. Applying LC_i here we find $\mathrm{LC}_i^{1'} G = \mathrm{LC}_i^{1'} \circ \mathrm{LC}_i^p \circ \mathrm{LC}_j^{p-1} \circ \ldots \circ \mathrm{LC}_j^1 (G) = \mathrm{LC}_j^{p-1} \circ \ldots \circ \mathrm{LC}_j^1 (G)$. Similarly to the above, each operation in the second orbit inverts an operation in the first orbit until we arrive back at the starting graph G. Hence, the second path, (begininning with LC_i is the reverse or the first.

□

This implies that only one trajectory need be considered in FINDACCESSIBLECLASSES. We henceforth always start the orbit with LC_j, which we will denote LC^k for the k^{th} LC of an orbit.

We now prove that such an orbit has period at most 6 for all graphs, independent of of the number of vertices.

Lemma 4. *Repeated application of LC on vertices i and j on some graph G has period at most 6, independent of the number of vertices.*

Proof. This is demonstrated independently in terms of edge-local complementation in [47], but we provide an alternate proof. Starting with some graph state $G = G^0$ let G^k be the graph state after k LC s. Next, we define three sets of vertices.

Firstly, The set of vertices which are in the neighbourhood of i, but not in the neighbourhood of j and excluding j and i, which we label

$$\mathcal{X}^k = \{N_{G^k}(i) - N_{G^k}(j) - \{j\} - \{i\}\}$$

Secondly, the intersection of vertices which are in the neighbourhood of i and the neighbourhood of j.

$$\mathcal{Y}^k = \{N_{G^k}(i) \cap N_{G^k}(j)\}$$

And finally the set of vertices which are in the neighbourhood of j, but not in the neighbourhood of i and excluding i and j.

$$\mathcal{Z}^k = \{N_{G^k}(j) - N_{G^k}(i) - \{i\} - \{j\}\}$$

Where for clarity we write $\mathcal{X}^0 = \mathcal{X}$, $\mathcal{Y}^0 = \mathcal{Y}$, $\mathcal{Z}^0 = \mathcal{Z}$. Now we can examine the effect of the LC orbit on a graph $G = G^0$.

Since i and j are always neighbours, the effect of LC_i on the k^{th} member of the orbit is to swap the sets $\mathcal{X}^k$ and $\mathcal{Y}^k$, and the effect of the LC_j is to swap sets $\mathcal{Y}^k$ and $\mathcal{Z}^k$, yielding the following, for $k = 1, \ldots, p$:

- For odd k, LC^k complements the subgraph induced by the sets $N_{G^k}(j) = \mathcal{Y}^k \cap \mathcal{Z}^k + \{i\}$, setting $\mathcal{Y}^{k+1} = \mathcal{Z}^k$ and $\mathcal{Z}^{k+1} = \mathcal{Y}^k$.
- For even k, LC^k complements the subgraph induced by the sets $= N_{G^k}(i) = \mathcal{X}^k \cap \mathcal{Y}^k + \{j\}$, setting $\mathcal{X}^{k+1} = \mathcal{Y}^k$ and $\mathcal{Y}^{k+1} = \mathcal{X}^k$.

By repeated application of the above rules, we find:

$$\mathcal{X}^6 = \mathcal{X} \qquad \mathcal{Y}^6 = \mathcal{Y} \qquad \mathcal{Z}^6 = \mathcal{Z}$$

We have shown the neighbourhoods of i and j have period at most 6. We have yet to show that the edges not involving i or j, have undergone one period, which will will do now.

We write the complementation of a graph as an operation on a graph $C : G \to G^{\mathsf{c}}$. Further, we denote the complementation of subgraph induced by a set of vertices, $\mathcal{A}$ as $C_{\mathcal{A}} : G \to G_{\mathcal{A}^{\mathsf{c}}}$, where $G_{\mathcal{A}^{\mathsf{c}}}$ is the input graph G but with the subgraph induced by the vertex set $\mathcal{A}$ complemented. We define $E[A,B]$ as the set of all bipartite edges in E that run from a vertex in the set A to a vertex in the set B, $E[\mathcal{A},\mathcal{B}] = \{(a,b) \in E \ : \ a \in \mathcal{A},\ b \in \mathcal{B},\ a \neq b\}$.

Also, we use $C_{E[A,B]} : G \to G_{E[A,B]^{\mathsf{c}}}$ do denote bipartite complementation. That is, $G_{E[A,B]^{\mathsf{c}}}$ is the input graph G but with the bipartite component between $\mathcal{A}$ and $\mathcal{B}$ complemented.

For odd k, LC^k performs the operation $C_{N_{G^k}(j)} = C_{\mathcal{Y}^k \cup \mathcal{Z}^k + \{i\}}$, whilst for even k, LC^k performs the operation $C_{N_{G^k}(i)} = C_{\mathcal{X}^k \cup \mathcal{Y}^k + \{j\}}$. To check the effect of the orbit on the edges of G^k we examine the graph operations in terms of fixed sets of vertices, namely $\mathcal{X}$, $\mathcal{Y}$, $\mathcal{Z}$, using the relations above. Hence the successive LC operations can be written in the following way:

$$\mathrm{LC}^1 \ = \ C_{\mathcal{Y} \cup \mathcal{Z} \cup \{i\}}, \qquad \mathrm{LC}^2 \ = \ C_{\mathcal{X} \cup \mathcal{Z} \cup \{j\}}, \qquad \ldots \qquad , \qquad \text{etc.}$$

Continuing to apply the rules, we find $\mathrm{LC}^l = \mathrm{LC}^{l+6}$. Hence after 12 successive LCs each complementation LC^l has cancelled with LC^{l+6} (since complementation of a fixed set of vertices commutes) and the graph has undergone one period.

Note $C_{\mathcal{A} \cup \mathcal{B}} = C_{\mathcal{A}} \circ C_{\mathcal{B}} \circ C_{E[A,B]}$. Using this expansion, the first six operations of the LC orbit can be written

$$\begin{aligned}
\mathrm{LC}^1 &= C_{\mathcal{Y}} \circ C_{\mathcal{Z}} \circ C_{E[\mathcal{Y},\{i\}]} \circ C_{E[\mathcal{Z},\{i\}]} \circ C_{E[\mathcal{Y},\mathcal{Z}]} \\
\mathrm{LC}^2 &= C_{\mathcal{X}} \circ C_{\mathcal{Z}} \circ C_{E[\mathcal{X},\{j\}]} \circ C_{E[\mathcal{Z},\{j\}]} \circ C_{E[\mathcal{X},\mathcal{Z}]} \\
\mathrm{LC}^3 &= C_{\mathcal{X}} \circ C_{\mathcal{Y}} \circ C_{E[\mathcal{X},\{i\}]} \circ C_{E[\mathcal{Y},\{i\}]} \circ C_{E[\mathcal{X},\mathcal{Y}]} \\
\mathrm{LC}^4 &= C_{\mathcal{Z}} \circ C_{\mathcal{Y}} \circ C_{E[\mathcal{Z},\{j\}]} \circ C_{E[\mathcal{Y},\{j\}]} \circ C_{E[\mathcal{Z},\mathcal{Y}]} \\
\mathrm{LC}^5 &= C_{\mathcal{Z}} \circ C_{\mathcal{X}} \circ C_{E[\mathcal{Z},\{i\}]} \circ C_{E[\mathcal{X},\{i\}]} \circ C_{E[\mathcal{Z},\mathcal{X}]} \\
\mathrm{LC}^6 &= C_{\mathcal{Y}} \circ C_{\mathcal{X}} \circ C_{E[\mathcal{Y},\{j\}]} \circ C_{E[\mathcal{X},\{j\}]} \circ C_{E[\mathcal{Y},\mathcal{X}]}
\end{aligned}$$

Noting $C_{E[\mathcal{B},\mathcal{A}]} = C_{E[\mathcal{A},\mathcal{B}]}$ (arguments of bipartite edges commute), $[C_{\mathcal{A}}, C_{\mathcal{B}}] = 0$ (complementations of a fixed set of vertices commute with one another) and $C_{\mathcal{A}} \circ C_{\mathcal{A}} = \mathbb{1}$ (complementation is self-inverse), we find $\mathrm{LC}^1 \circ \mathrm{LC}^2 \circ \mathrm{LC}^3 \circ \mathrm{LC}^4 \circ \mathrm{LC}^5 \circ \mathrm{LC}^6 = \mathbb{1}$ since each complementation is performed twice. Hence LC operations on only two vertices have period six.

□

1.2 FINDACCESSIBLECLASSES Algorithm

Algorithm 1: FINDACCESSIBLECLASSES

Data: A resource graph $G(E,V)$ of order n
A function generating graphs of allowed qubit interactions, $t \in T$
The set of sets of entanglement classes of order n, S^n
Convergence criteria, d, the proportion of iterations to be run since the last novel class was found

Result: Outputs the indices of LU classes of that are accessible with a given resource, $G(E,V)$, using only postselected fusion and CZ^{LO} gates, as well as a recipes for each.

$\mathcal{L}'_R, H^R, P^R \leftarrow \emptyset$ // H will be the recipe for each class, indexed by class
$j \leftarrow 0$ // L' are the classes which can be accessed
$G \leftarrow R$
while $c < d \cdot j$ **do** // Stop when convergence ratio is reached
  $p \leftarrow 1$ // Success probability of this this experiment
  $j \leftarrow j+1$ // Number of iterations done so far
  $t(E,V) \leftarrow$ RANDMEMBER(T) // Choose an ordered gate topology from the allowed set T
  $L \leftarrow$ RANDINT$(n-1-|E[G]|, |E[t]|)$ // L is the number of gates to perform from the tree
  for $i \leftarrow 1$ **to** L **do**
    $r \leftarrow$ RANDMEMBER$(E[t])$ // Choose the next edge from the gate topology
    $g_r \leftarrow$ RANDMEMBER$(\{F_r, CZ_r^{LO}\})$ // we will apply either CZ or fusion along the chosen edge
    Apply g_r to $G(E,V)$ // Apply the gate
    Append "g_r" to h // Save what we have done to the recipe index
    if $g = CZ^{LO}$ **then**
      $p \leftarrow p \times (1/9)$ // Keep track of success probability
      $m \leftarrow$ RANDINT$(0,5)$ // LC periodic with period 6 for two vertices
      for $k \leftarrow 1$ **to** m **do**
        $\alpha \leftarrow r_{(1+k \pmod 2)}$ // Want to apply LC alernatingly to i, j, i, etc.
        $G(E,V) \leftarrow \mathrm{LC}_\alpha(G(E,V))$ // Apply LC
        Append "LC_α" to h // Save what has been done to the recipe
      end
    if $g = F$ **then**
      $p \leftarrow p \times (1/9)$ // Keep track of success probability
      $m \leftarrow \mathrm{rand}(0,14)$ // the Width of largest LC class is 14
      for $k \leftarrow 1$ **to** m **do**
        $\alpha \leftarrow$ RANDMEMBER$(V_G[N_G(i) \cup N_G(i) + \{i\} + \{j\}])$ // LC does not commute with F
        $G(E,V) \leftarrow \mathrm{LC}_\alpha(G(E,V))$ // Hence need to LC whole union of neighbourhoods of i, j
        Append "LC_α" to h // Save what has been done to the recipe
      end
  end
  if $G(E,V)$ *is not equivalent to any graph in classes* $\mathcal{L}'_R$ **then** // Did we find a new class of graph?
    Append i to $\mathcal{L}'_R$ where S_i^n is the equivalence class of $G(E,V)$ // Save which class we accessed
    $H_j^R \leftarrow h$ // Save successful recipe
    $P_j^R \leftarrow p$ // Save success probability
    $c \leftarrow j$ // Keep track of convergence criteria
  else if $p > P_j^R$ *and* $G(E,V)$ $\mathcal{L}_{R'_j}$ *is equivalent to* $G(E,V)$ $\mathcal{L}_{R'_j}$ **then**
    Replace H_j^R with h // Save imrpoved recipe
    Replace P_j^R with p // Save imrpoved probability
end
Return $\{\mathcal{L}'_R, H\}$

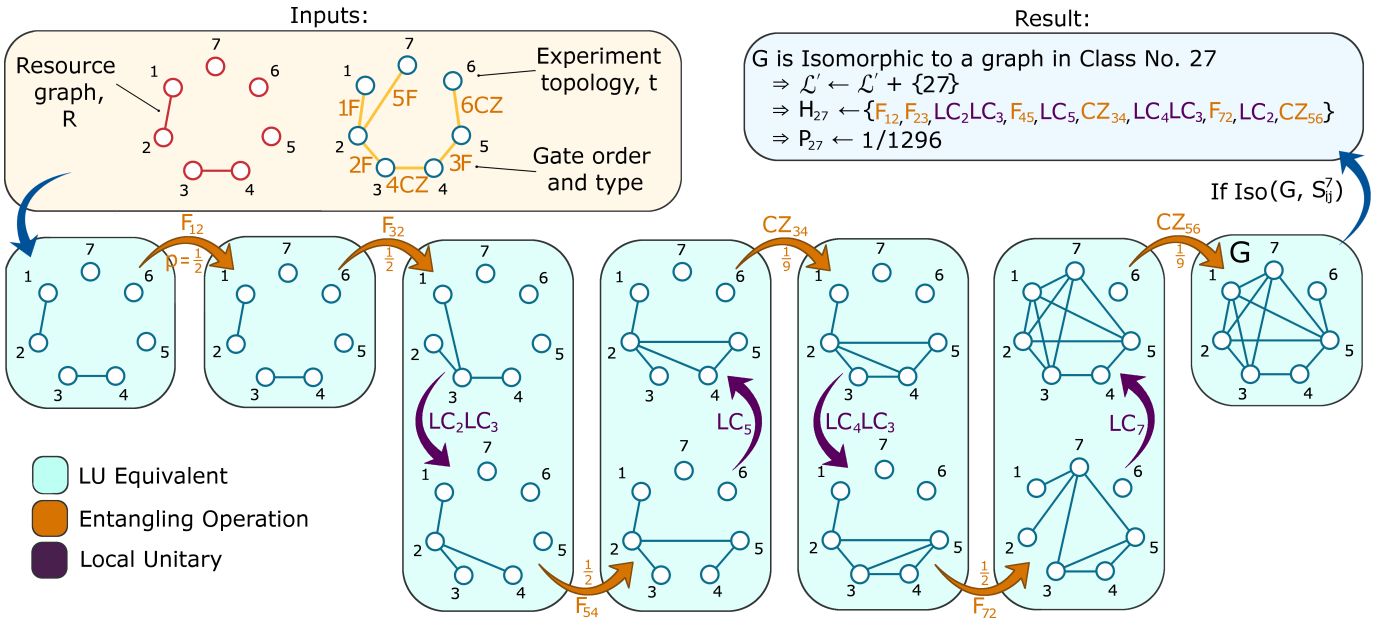

Figure 7: An alternate example of one Monte Carlo iteration of FINDACCESSIBLECLASSES. Starting from a given resource state, in this case 7 single photons, operations for experiment topology are performed in order, interspersed with relevant LCs on the previously acted upon vertices. Pairs of qubits populated with photons from EPPs are highlighted in pink. If the resulting graph is not isomorphic to any graph found thus far, the entanglement class of the graph i is saved to a set $\mathcal{L}'_R$. After many runs, $\mathcal{L}'_R \approx \mathcal{L}_R$.

1.3 Enumeration of Graph States

n	9-Photon resource state, R	Indices of LU classes accessed, $\mathcal{L}'_R$	$\lvert\mathcal{L}'_R\rvert/\lvert S^9\rvert$
9	4 non-degenerate EPP and one single photon	148 to 197, 199, 200, 204 to 208, 212, 214, 218, 219, 221, 222, 225, 227, 233 to 235, 238, 241, 247, 249 to 251, 256, 259 to 260, 263, 272, 274, 275, 297, 328, 392, 410	$85/440 \approx 0.19$
9	Nine single photons	148 to 200, 202, 204 to 208, 211, 212, 214 to 215, 218, 219, 221 to 222, 225, 227 to 229, 233 to 235, 237 to 238, 241, 247, 249 to 251, 256, 259, 260, 262, 263, 271 to 275, 290, 297, 299, 301, 305, 319, 328, 329, 342, 346, 388, 392, 401, 41	$104/440 \approx 0.24$
9	Four pairs and one single photon	148 to 558, 560 to 567, 569 to 572, 575 to 578, 581, 584, 586, 587	$431/440 \approx 0.98$

Table 2: Classes of graph state which can be generated using PEGs given different 9-qubit resource states R, written $\mathcal{L}_R$. These classes (denoted S_i^n) are indexed starting from the 2-vertex graph state. See Supplementary Material 1.3 for a complete list of graph states indexed up to 8 vertices (from refs. [30, 34, 40]). This table was generated by FINDACCESSIBLECLASSES.

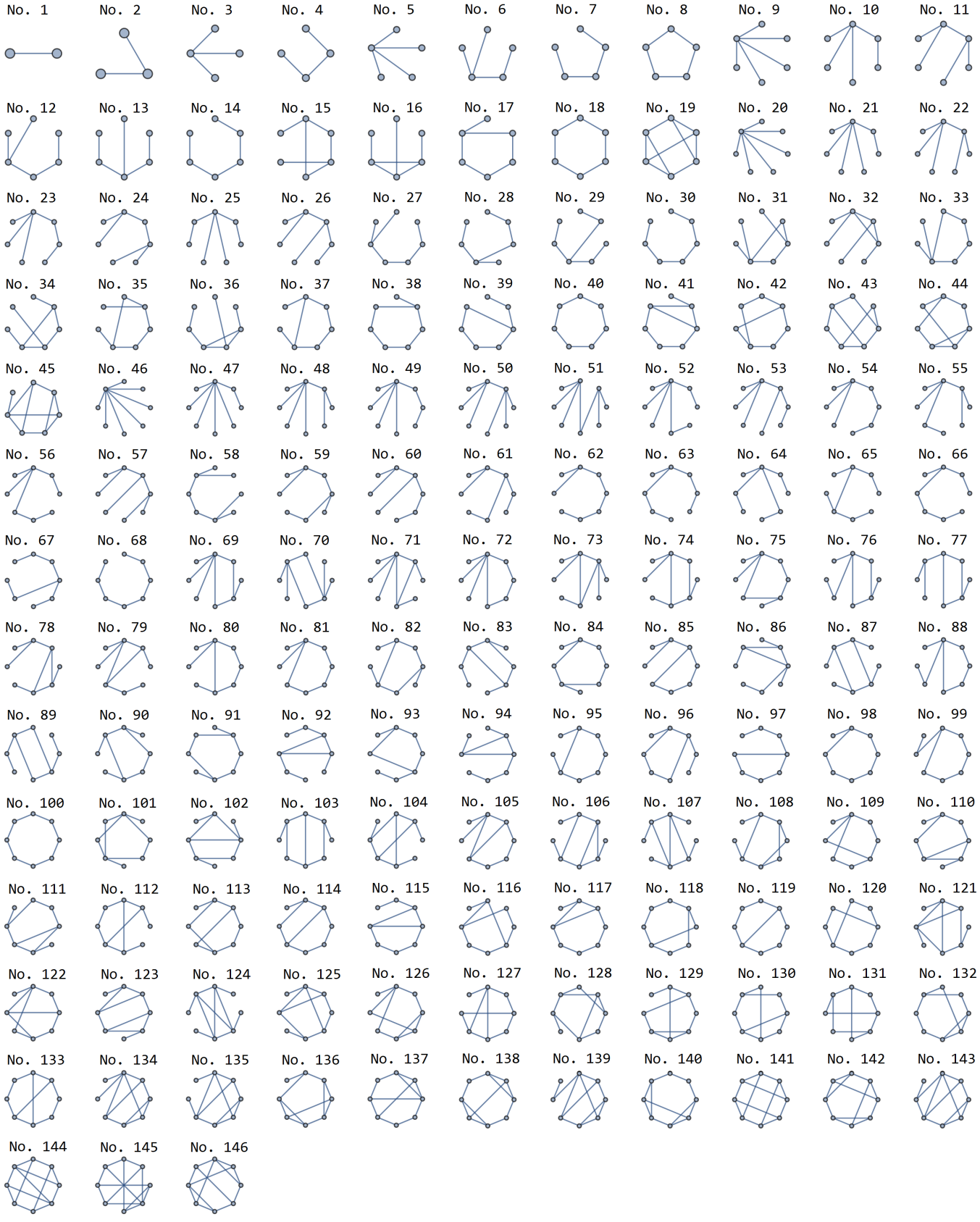

Figure 8: Minimal edge count representatives from each of the LU classes up to 8 qubits, canonically numbered as in ref. [30, 34, 40].

1.4 Example of postselected gate - CZ

The postselected CZ^{LO} acting on $|{+}{+}\rangle$ produces the following state:

$$\begin{aligned}\mathrm{CZ}^{LO}|++\rangle =&\frac{1}{3}|101000\rangle_f+\frac{1}{3\sqrt{2}}|100100\rangle_f-\frac{1}{3\sqrt{2}}|100010\rangle_f\\&+\frac{1}{3}|100001\rangle_f+\frac{1}{3\sqrt{2}}|011000\rangle_f+\quad\frac{1}{6}|010100\rangle_f\\&+\frac{1}{6}|010010\rangle_f+\frac{1}{3\sqrt{2}}|010001\rangle_f+\quad\frac{1}{6}|001100\rangle_f\\&-\frac{1}{6}|001010\rangle_f-\frac{1}{3\sqrt{2}}|001001\rangle_f-\frac{1}{3\sqrt{2}}|000110\rangle_f\\&+\frac{1}{3}|000101\rangle_f-\quad\frac{1}{3}|002000\rangle_f+\quad\frac{1}{3}|000200\rangle_f\end{aligned}$$

Where the non-qubit terms in

$$\begin{aligned}\mathcal{J}=\mathrm{span}(&|101000\rangle_f,|100100\rangle_f,|100010\rangle_f,\\&|100001\rangle_f,|011000\rangle_f,|010001\rangle_f,\\&|001001\rangle_f,|000110\rangle_f,|000101\rangle_f,\\&|002000\rangle_f,|000200\rangle_f)\end{aligned}$$

are removed by postselection P_{Q}. Hence

$$\begin{aligned}P_{\mathrm{Q}}\mathrm{CZ}^{LO}|++\rangle=&\frac{1}{6}|010100\rangle_f+\frac{1}{6}|010010\rangle_f\\&+\frac{1}{6}|001100\rangle_f-\frac{1}{6}|001010\rangle_f\\=&\frac{1}{6}|00\rangle+\frac{1}{6}|01\rangle+\frac{1}{6}|10\rangle-\frac{1}{6}|11\rangle\\=&\frac{1}{3}\mathrm{CZ}|++\rangle\end{aligned}$$

1.5 Postselection of multiple entangled pairs from squeezed vacuum

Pairwise entangled states of n pairs of photons are commonly generated by two postselecting the n-photon subspace of $\frac{n}{2}$ coherently pumped EPP source. Unfortunately, these states contain junk states affect postselectability. This is because it is not possible to distinguish the case where there were one pair of photons is generated in each source, and the case where when some sources produce more than one pair, which is at least as likely (for n photons in total). To see this, take two (unnormalised) fock states produced by a EPP source.

$$\begin{aligned}|\xi\rangle^{\otimes 2}=(&|0000\rangle+\gamma|1010\rangle+\quad\gamma|0101\rangle+\\&\gamma^2|2020\rangle+\gamma^2|0202\rangle+\ldots)^{\otimes 2}\end{aligned}$$

Where $|\Phi^+\rangle=|1010\rangle_f+|0101\rangle_f$ for two pairs of two modes comprising two qubits. The $O(\gamma^2)$, four-photon terms:

$$\begin{aligned}|\xi\rangle^{\otimes 2}=&\gamma^2|\Phi^+\Phi^+\rangle+\gamma^2|11110000\rangle+\gamma^2|20200000\rangle\\&+\gamma^2|02020000\rangle+\gamma^2|00001111\rangle+\gamma^2|00002020\rangle\\&+\gamma^2|00000202\rangle\end{aligned}$$

The postselected state, $|\Phi^+\Phi^+\rangle$ makes up only a minority of the four photon state, and two-photon-per-qubit terms dominate. Similarly, for larger ensembles of sources, each permutation of pairs being produced the sources is present in the superposition, and must be considered. For example, in the six photon subspace of three sources, there are terms where all three pairs were produced in just one source, as well as terms where just one source produced an extra pair. Postselected sources produce mostly junk states, and how these traverse and experiment must be considered when evaluating whether an experiment will successfully postselect.